Influence of fuel Lewis number on flame-wall interaction for impinging turbulent premixed flames

Ilias Konstantinou, Umair Ahmed, Nilanjan Chakraborty
School of Engineering, Newcastle University Newcastle-Upon-Tyne NE1 7RU, UK

1 Introduction

The fundamental understanding of the combustion phenomena taking place in the vicinity of walls remains limited. This can be attributed to the fact that flame quenching occurs at only a few micrometers away from the wall posing a challenge from both an experimental and computational point of view. The interaction of the flame with the walls plays a key role in determining the lifespan of the combustors. With the current trend in the automotive and aerospace industries pushing towards smaller combustors, the phenomenon of flame-wall interaction (FWI) is becoming increasingly important due to its implications on pollutant formation and flame stability. Moreover, heat generation introduced by combustion processes gives rise to thermal stresses which originate from fluctuations in the wall temperature. A better understanding of the physics behind FWI is necessary for the design of the next generation combustion engines at industrial scales which are expected to run on a range of fuels with different Lewis numbers, Le. However, relatively little effort has been directed in the study of FWI at different Le. In the current work, Direct Numerical Simulations (DNS) of statistically planar flames impinging on isothermal inert walls have been carried out to analyse the influences of non-unity fuel Lewis number, Le_F, on different aspects of FWI. Statistical behaviours of the wall heat flux, wall-normal strain rate and dilatation rate have been analysed for different values of Le_F and turbulence intensities under isothermal wall boundary conditions.

2 Problem Description and Numerical Implementation

Direct Numerical Simulation of wall impingement of statistically planar turbulent premixed flames at different Le_F and turbulence intensities have been performed. The Lewis number, Le_i, is defined as the ratio of the thermal, α_i, to molecular diffusivity, D_i, where i is the species in the gas mixture. Three different values of $Le_F = 0.8, 1.0, 1.2$ at three different turbulence intensities of $u'/S_L = 1.0, 2.0, 5.0$ are analysed, as shown by Fig. 1. A fully compressible code SENGA [1] has been used for conducting the simulations which makes use of a 10^{th} order central difference scheme for the spatial discretisation which decreases to a one-sided 2^{nd} order scheme at the non-periodic boundary nodes. A low storage 3^{rd} order explicit Runge-Kutta scheme is adopted for the time advancement of the solution. Figure 1 schematically illustrates the configuration of the computational domain. The no-slip condition is enforced at the isothermal inert wall where the wall temperature is taken to be the unburned gas temperature, T_u. The wall-normal mass flux is taken to be zero. Following the Navier-Stokes Characteristic Boundary Conditions (NSCBC) formulation of [2], a partially non-reflecting outflow boundary condition is specified in the x_2-direction, while periodicity is used in the x_3-direction. A precursor simulation was used to evolve the turbulent velocity

Correspondence to: i.konstantinou@newcastle.ac.uk

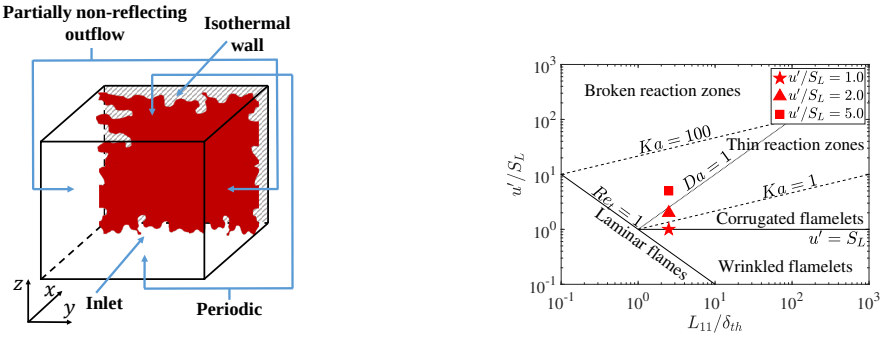

Figure 1: Schematic diagram of the computational domain for the impinging statistically planar turbulent premixed flame configuration (left). Combustion regimes diagram for the present study (right).

field by scanning a homogeneous isotropic turbulent field generated *a priori* based on a prescribed energy spectrum [3]. The thermal flame thickness, $\delta_{th} = (T_{ad} - T_u)/max|\nabla \hat{T}|_L$ (where $\hat{T}$, T_u and T_{ad} are the instantaneous, unburned and adiabatic flame temperatures, respectively) is resolved by 10 grid points for all flames considered here. A single step Arrhenius-type chemical mechanism is employed for computational economy. The computational domain is discretised using a uniform Cartesian mesh of $180 \times 252 \times 180$ grid points which translates to $37.51\delta_Z \times 52.60\delta_Z \times 37.51\delta_Z$ in terms of the Zel'dovich flame thickness, $\delta_Z = \alpha/S_L$, where S_L is the unstretched laminar burning velocity. All simulations have been carried out for at least 4 throughpass times (i.e. $t_{sim} \geq 4L_{domain}/U_b$) by which a reasonably statistically stationary stage has been achieved. Table 1 summarises the simulation parameters for each of the cases and their nominal po-

Table 1: Simulation parameters for flames of varying fuel Lewis number, Le_F.

Case	A1	A2	A3	B1	B2	B3	C1	C2	C3
Le_F	0.8	0.8	0.8	1.0	1.0	1.0	1.2	1.2	1.2
u'/S_L	1.0	2.0	5.0	1.0	2.0	5.0	1.0	2.0	5.0
Ka	0.6	1.8	7.1	0.6	1.8	7.1	0.6	1.8	7.1
Da	2.5	1.3	0.5	2.5	1.3	0.5	2.5	1.3	0.5

sition on the regime diagram is shown in Fig. 1. The Kolmogorov length scale, η, is approximately 5.5 (for A1, B1 & C1), 3.3 (for A2, B2 & C2) and 1.7 (for A3, B3 & C3) times the grid spacing. The integral length scale to thermal flame thickness ratio, $l_t/\delta_{th} = 2.5$, and bulk velocity to flame speed ratio, $U_b/S_L = 6.0$, were kept constant for all cases. Standard values for the Zel'dovich number, $\beta = T_{ac}(T_{ad} - T_u)/T_{ad}^2 = 6.0$ (where T_{ac} is the activation temperature), Prandtl number, $Pr = 0.7$, and ratio of specific heats, $\gamma = 1.4$, were used in all simulations and the oxidiser Lewis number, Le_O, was kept at unity. The air-fuel mixture chosen in this study is representative of methane-air mixture at stoichiometric conditions. The heat release parameter was set to $\tau = (T_{ad} - T_u)/T_u = 3.0$ and is identical for all flames. The Karlovitz and Damköhler numbers are defined as $Ka = (u'/S_L)^{1.5}(l_t/\delta_{th})^{-0.5}$ and $Da = (l_t S_L)/(\delta_{th} u')$, respectively.

3 Results and Discussion

Instantaneous three-dimensional realisation of the reaction progress variable, c, isosurfaces are shown in Fig. 2 at varying Le_F for $u'/S_L = 5.0$ at the same time instant. The reaction progress variable can be

defined in terms of fuel mass fraction, Y_F, as $c = (Y_{F,u} - Y_F)/(Y_{F,u} - Y_{F,b})$ where the subscripts u and b refer to the unburnt and burnt gases. Accordingly, c monotonically increases from zero (fresh gas side) to unity (burnt gas side). It can be seen from Fig. 3 that $c \neq T$ (where $T = (\hat{T} - T_u)/(T_{ad} - T_u)$ is the non-dimensional temperature) in the vicinity of the wall for all cases but the equality between c and T is maintained for $Le_F = 1.0$ case away from the wall. Figure 3 shows that temperature drops in the vicinity of the wall due to wall heat loss, which gives rise to local flame quenching, as can be substantiated from the broken contours of the normalised fuel reaction rate magnitude $|\dot{\omega}_F| \times \delta_Z/\rho_u S_L$ (for this thermo-chemistry heat release rate is directly proportional to the fuel reaction rate magnitude). It can further be seen from Fig. 3 that the elements of c isosurfaces, which are concave (convex) towards the reactants exhibit low (high) values of the normalised fuel reaction rate magnitude $|\dot{\omega}_F| \times \delta_Z/\rho_u S_L$ due to the combination of strong defocussing (focussing) of fuel and weak focussing (defocussing) of heat in the $Le_F = 0.8$ case. Just the opposite mechanism is responsible for relatively high values of $|\dot{\omega}_F| \times \delta_Z/\rho_u S_L$ in the regions of c isosurfaces which are concave towards the reactants in the $Le_F = 1.2$ case. Furthermore, Fig. 3 also reveals that the flame in the $Le_F = 1.2$ case is pushed closer to the wall by the upstream flow in comparison to the corresponding $Le_F = 0.8$ and $Le_F = 1.0$ cases because the flame propagation rate into the reactants (and thus also the turbulent flame speed) decreases with increasing Le_F.

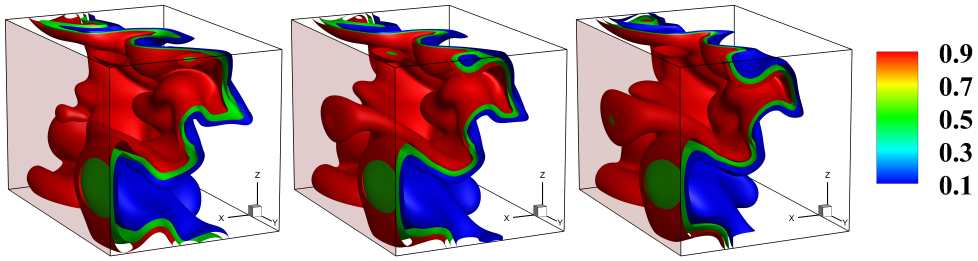

Figure 2: Instantaneous realisation of c isosurfaces for cases A3 (left), B3 (centre) and C3 (right).

In this study, the distance from the wall to the flame front is calculated by tracking the isosurfaces corresponding to the non-dimensional temperature, $T = 0.9$, and the reaction progress variable, $c = 0.9$, which are denoted as $\delta_{T=0.9}$ and $\delta_{c=0.9}$, respectively. Figure 4 shows the joint probability density function (PDF) between $\delta_{T=0.9}/\delta_Z$ and normalised wall heat flux, $Q_W^+ = Q_W/[\rho_u S_L C_{P,u}(T_{ad} - T_u)]$ where the superscript $+$ denotes a non-dimensional quantity, with Q_W being the dimensional wall heat flux and $C_{P,u}$ being the specific heat capacity at constant pressure of the unburnt gases. As the flame approaches the isothermal cold wall, the wall heat flux magnitude increases which consequently makes the flame temperature decrease at the flame front due to heat losses. The critical normalised flame-wall distance (at which the flame quenching process starts to occur and Q_W assumes its maximum value) is found to be $\delta_{T=0.9}/\delta_Z = 3.8$ and the corresponding maximum wall heat flux magnitude is $Q_W^+ = 0.36$ for $Le_F = 1.0$ cases with $u'/S_L = 2.0$. This compares well with the findings of [5] for similar flow configuration and turbulence intensity $(u'/S_L = 2.0)$ for $Le_F = 1.0$. However, for the $Le_F = 1.2$ $(Le_F = 0.8)$ case, the critical flame-wall distance is found to be 3.0 (3.8) where the maximum wall heat flux magnitude assumes a value of $Q_W^+ = 0.36$ (0.37) for $u'/S_L = 2.0$. As the flame elements, which are concavely curved towards the reactants (see Fig. 3), exhibit higher temperatures in the $Le_F = 1.2$ case, and the flame is pushed closer to the wall, the smallest distance for which the combustion process in the $Le_F = 1.2$ case can be sustained without quenching remains smaller than in the corresponding $Le_F = 0.8$ and 1.0 cases. By contrast, in the $Le_F = 0.8$ case the flame quenches more readily at a distance higher than the other corresponding cases because of the relative proximity of the low temperature regions (which are concavely curved towards the reactants) closer to the wall.

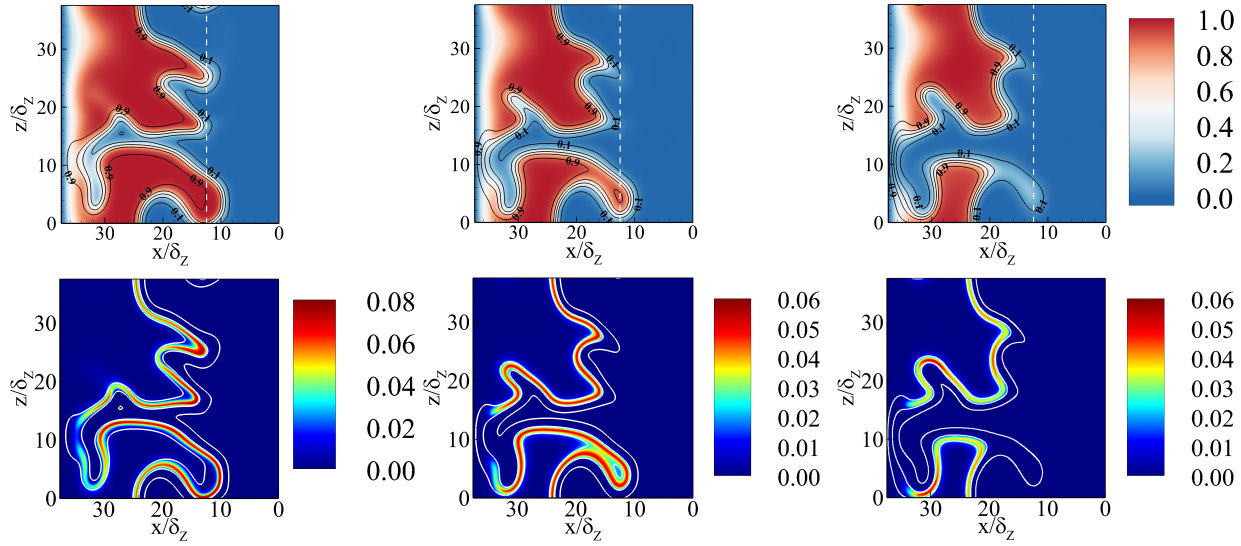

Figure 3: Contour lines of c superimposed with the instantaneous realisation of the non-dimensional temperature, T (vertical dashed line denoting the initial position of the $c = 0.5$ isosurface) (top), and non-dimensional fuel reaction rate, $|\dot{\omega}_F| \times \delta_Z/\rho_0 S_L$ (the corresponding $c = 0.1, 0, 5$ and 0.9 levels are shown) (bottom) on the $x - z$ plane at $y/\delta_Z = 22.22$ for case A3 (left), B3 (centre) and C3 (right).

This gives rise to a decrease in the critical quenching distance, which eventually leads to an increase in the maximum value of Q_W^+ with increasing Le_F. At higher (lower) turbulence intensity, the distribution of the

Table 2: Wall heat fluxes and the corresponding quenching distances.

Case	A1	A2	A3	B1	B2	B3	C1	C2	C3
Q_W^+	0.33	0.37	0.44	0.32	0.36	0.48	0.30	0.36	0.40
$\delta_{T=0.9}/\delta_Z$	4.3	3.8	3.2	4.3	3.8	3.4	3.5	3.0	2.2

wall heat flux spreads wider (shrinks) hinting that the flame breaks (thickens) and parts of it detach resulting in higher probability of finding regions with lower (greater) Q_W^+. The overall trend of the flame is to attain a lower flame-wall distance for $Le_F > 1.0$ values which holds true for all the turbulence intensities investigated here, as it is shown in Fig. 3 where the flame manages to reach closer to the wall at $Le_F = 1.2$. Table 2 collectively presents the wall heat fluxes and the corresponding quenching distances. The joint PDF between Q_W^+ and the normalised strain rate in the wall-normal x_1-direction, $\partial u_1/\partial x_1|_W \times \delta_Z/S_L$ is provided in Fig. 5. For the lower turbulence intensity cases of $u'/S_L = 1.0$, the overall trend of $\partial u_1/\partial x_1|_W \times \delta_Z/S_L$ is negative which is typical of a counterflow configuration. In the case of higher turbulence intensity, it is found that $\partial u_1/\partial x_1|_W \times \delta_Z/S_L$ aligns along the zero axis indicating that the stagnation bubble ahead of the wall increases in size with increasing turbulence intensity due to enhanced momentum exchange. The wall-normal strain rate proves to be insensitive to the changes in Le_F as the normal strain rate behaviour is principally determined by background fluid motion which is not significantly affected by the thermo-diffusive effects induced by non-unity Le_F. Figure 6 shows the joint PDF between the dilatation rate, $\Delta = \partial u_i/\partial x_i$, on the $c = 0.9$ isosurface normalised by δ_Z/S_L and the normalised flame-wall distance, $\delta_{c=0.9}/\delta_Z$. The variation of dilatation rate in the case of FWI is determined primarily by two competing

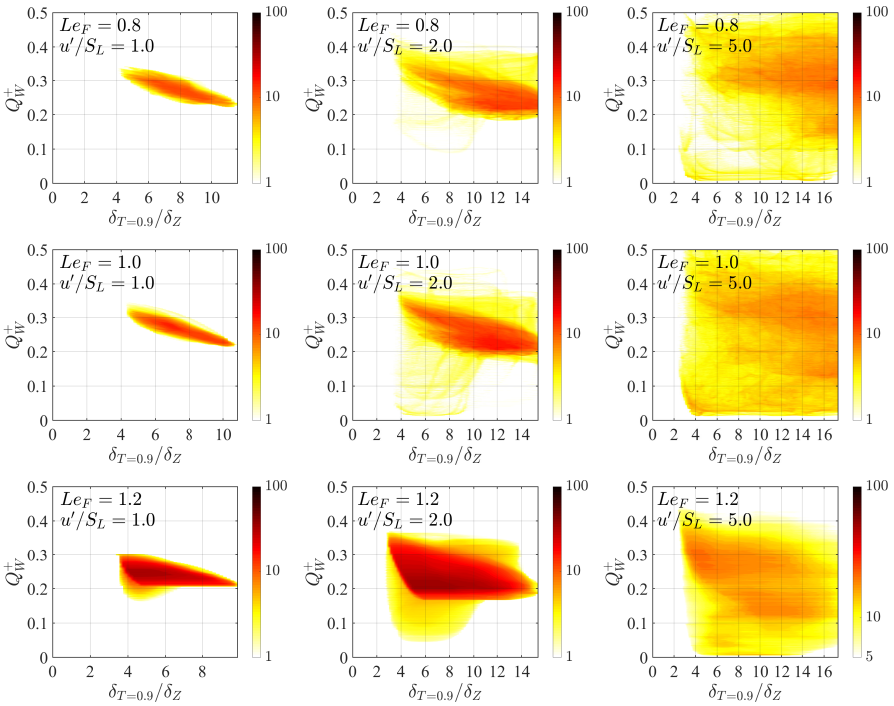

Figure 4: Joint PDFs between the normalised wall heat flux, Q_W^+ and the flame-wall distance, $\delta_{T=0.9}/\delta_Z$.

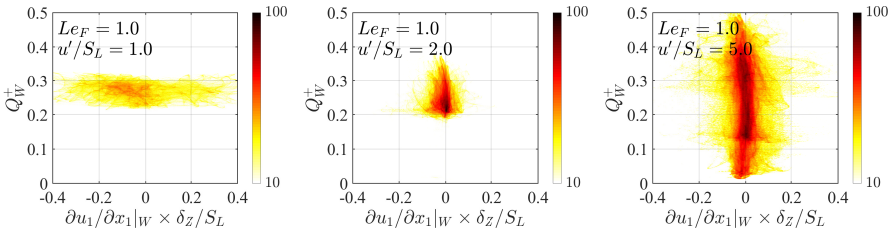

Figure 5: Joint PDFs between the wall heat flux, Q_W^+ and the wall-normal strain rate, $\partial u_1/\partial x_1|_W \times \delta_Z/S_L$.

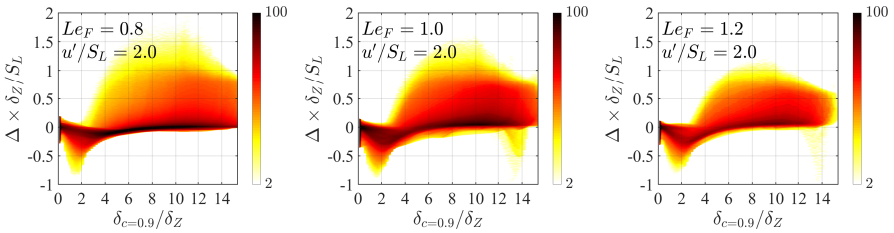

Figure 6: Joint PDFs between the dilatation rate, $\Delta \times \delta_Z/S_L$ and the flame-wall distance, $\delta_{c=0.9}/\delta_Z$.

effects; heat loss owing to the presence of the cold isothermal wall, and heat generation due to combustion. In essence, zero Δ is interpreted as the flame region where the two aforementioned effects balance each other out. As the flame approaches the wall, Δ in the $Le_F = 1.0$ case achieves a minimum value of -0.78 for $u'/S_L = 2.0$ likewise in the case of [5] which is also true for the corresponding $Le_F = 0.8$ case, whereas for the corresponding $Le_F = 1.2$ case Δ shows a minimum of -0.65. Note for the $Le_F = 0.8$ and 1.0 cases, the $\Delta = 0$ point takes place at $\delta_{c=0.9}/\delta_Z \approx 2.9$, whilst for the corresponding $Le_F = 1.2$ case this is achieved at a distance further away from the wall, i.e. $\delta_{c=0.9}/\delta_Z \approx 3.7$. The overall trend and shape of the joint PDF between $\Delta \times \delta_Z/S_L$ and $\delta_{c=0.9}/\delta_Z$ remain similar for the other two turbulence intensities because the statistical behaviour of $\Delta \times \delta_Z/S_L$ is principally determined by thermo-chemical processes which remain qualitatively similar for the range of u'/S_L considered here.

4 Conclusions

In the present study, the effects of fuel Lewis number, Le_F, have been investigated for FWI of statistically planar turbulent premixed flames impinging on inert isothermal walls for different turbulence intensities. The critical quenching distance has been found to decrease with increasing Le_F in this configuration. By contrast, the maximum wall heat flux magnitude remains comparable for all Le_F values considered here. Similar behaviour has been observed for increasing turbulence intensity where flame-wall distance of up to $\delta_{T=0.9}/\delta_Z \approx 2.2$ has been obtained. No strong correlation is found between the wall heat flux and the wall-normal strain rate with varying Le_F. However, it has been found that the distribution of the wall heat flux in regions of non-zero wall-normal strain rate is altered at different turbulence intensities. The joint PDFs between dilatation rate and wall-normal distance have been marginally affected by the variation of Le_F, with the overall trend remaining qualitatively similar for different turbulence intensities. It is worth noting that the findings in this work are expected to remain qualitatively similar in the case of flames with variable transport properties and detailed chemical mechanism. It has recently been shown that the underlying fluid mechanics is not affected by a detailed chemical mechanism and temperature dependent transport properties [6]. Minor differences have been observed in the case of a multi-step chemical mechanism in a HOQ configuration by [7] where a non-zero value of heat release rate was observed at the wall during FWI. However, further investigation of FWI with detailed chemistry forms part of the ongoing work and will be reported in future investigations.

Acknowledgements

The authors are grateful to EPSRC (No. EP/P022286/1) for the financial support. Computational support was provided by ARCHER (No. EP/K025163/1) and Rocket (Newcastle University).

References

[1] Jenkins KW, Cant RS. (1999). Recent Advances in DNS and LES. 191-202.

[2] Yoo CS, Im HG. (2007). Combust. Theor. Model. 11:259.

[3] Rogallo RS. (1981). NASA Technical Memorandum. 81315.

[4] Poinsot T, Veynante D. (2005). 2^{nd} ed. Edwards.

[5] Zhao P, Wang L, Chakraborty N. (2018). J. Fluid Mech. 848:193.

[6] Ahmed U, Doan NAK, Lai J, Klein M, Chakraborty N, Swaminathan N. (2018). Phys. Fluids, 30(10):105102.

[7] Lai J, Klein M, Chakraborty N. (2018). Flow, Turb. Combust. 101(4):1073-1091.